Behavior of Full-scale Frames with Slim Floor Slab Construction under Exposure in a Fire Resistance Furnace

YULI DONG*

School of Civil Engineering, Harbin Institute of Technology, China

KULDEEP PRASAD

National Institute of Standards and Technology Gaithersburg, MD, USA

ABSTRACT: In recent years, there has been increasing interest in developing and designing slim floor systems in steel-framed buildings. This article describes the results of a furnace test conducted on two full-scale composite steel frames with slim floor slab construction to understand their performance under fire loading. In one frame, the beam-to-column connections were protected, while in the second frame, the columns as well as the beam-to-column connections were protected. During the test, the furnace temperature, the steel and concrete temperature, as well as the horizontal and vertical displacements were recorded. The complete deformation process of the test frame observed during the heating phase and the cooling phase, including failure of the frame, is described in this article. A comparison of the data obtained from the two tests indicates that the fire resistance of a composite beam is significantly better than that of a steel column. Fire resistance of composite frames with slim floor slabs is compared with data on a conventional floor slab. Results indicate that the fire resistance rating of frames constructed with slim floor slabs is at least as good as that of frames with conventional floor slab construction.

KEY WORDS: slim floor, structural failure, furnace heating, composite steel frame, fire resistance.

INTRODUCTION

INCREASING INTEREST IN designing slim floor systems for steel framed buildings in recent years has increased the need to evaluate their performance under fire loading. In the slim floor system, the steel beam is

*Author to whom correspondence should be addressed. E-mail: dongyl@hit.edu.cn

1042-3915/09/03 0197–24 $10.00/0 DOI: 10.1177/1042391509104183

SAGE Publications, Los Angeles, London, New Delhi and Singapore

contained (at least partially) within the depth of the concrete floor or composite slab [1–4]. Compared with the conventional composite frame system that has a primary- secondary -beam system, the slim floor frame has a different structural form, where the secondary beam is the same as the primary beam. In a conventional composite frame, the floor beam is under the concrete slab, while in the slim floor frame the upper part of beam is encased by the concrete slab. Therefore, slim floor construction achieves a minimum depth of the floor and offers significant savings in construction cost.

There has been little work to date on understanding the fire resistance of full-scale composite steel frame systems [5–13]. Since slim floor slab construction is a relatively new type of construction, fire resistance data for slim floor slab construction is extremely limited [1,2]. Traditionally, the fire resistance of construction steelwork has been investigated by conducting standard fire tests. Most of the fire tests to date have been performed on single isolated structural members (i.e., steel beams, composite beams, concrete floor slabs) subjected to furnace heating [9–12]. The British Standards Institution [9] compiled a large number of the UK's standard fire resistance test results on steel structures. Franssen et al. [10] have reported a database containing many column fire tests. In such tests involving single isolated elements, many aspects of structural behavior that occur due to the interaction between adjacent members cannot be studied [14,15]. Performance of real structures subject to fires can sometime be much better than that predicted from standard tests due to structural continuity and the interaction between members.

The authors have previously described an experimental study [16,17] evaluating the behavior of two full-scale composite steel frames with conventional floor slab construction under furnace loading. For these tests, in one test frame, the beam-to-column connections were protected from furnace heating with an alumino-silicate refractory fiber blanket, while in the second frame the columns as well as the beam-to-column connections were protected. A comparison of the data obtained from the two tests indicated that the fire resistance of a composite beam was significantly better than that of a steel column. It was proposed that in certain engineering design scenarios using similar elements and connections, the composite beam may not have to be protected due to its higher fire resistance rating, while the steel column should be protected from fire exposure. The experiments described in the current article differ from those described in [16,17] in the construction of the test frame. In [16,17], a conventional floor slab construction was studied, while in the current article, experimental data for fire resistance of a slim floor slab construction will be discussed.

In order to evaluate the structural performance under fire loading of a slim floor slab construction, two tests were conducted on full-scale steel

frames subjected to different heating conditions. The construction of the test assembly and the furnace is described in the following section, focusing on the differences between the current tests and those that were reported in [16,17]. The major experimental results including thermocouple temperature measurements and transducer displacement data for both the columns and the composite beam have been provided. Photographic evidence of the failure modes observed in the two tests is presented and an explanation is provided for the observed behavior. The results of this study are compared and contrasted with those reported in [16,17], to understand the differences in the observed structural response, for slim floor and conventional floor slab construction under fire loading.

Material properties test results for steel and concrete are not included here because many such tests of similar materials have been conducted in China, and these experimental results can be used to analyze the current frame tests.

FRAME CONSTRUCTION AND FURNACE TEST CONDITIONS

The test frame shown in Figure 1 is a single-story, one-bay, 2D, sway portal frame with fixed bases. The frame was very similar in construction to that described in [16,17]. The test frame consists of two columns that

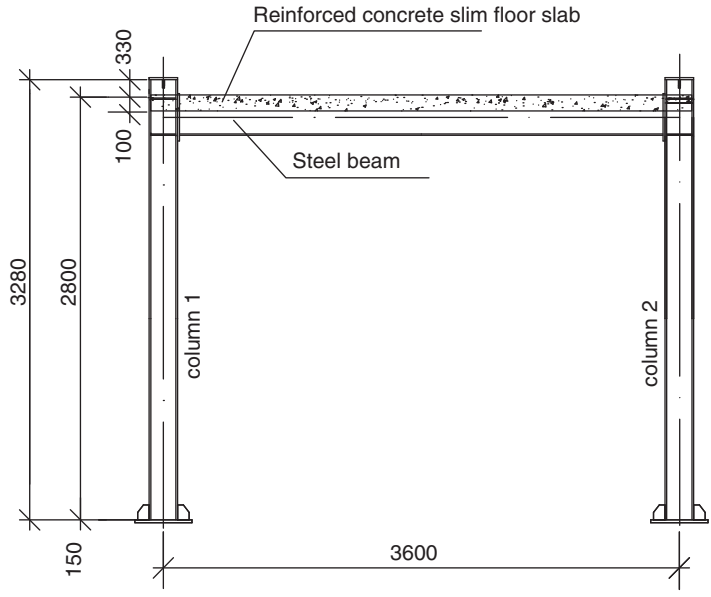

Figure 1. *Construction of a single story, one bay, 2D, sway portal frame with fixed bases for furnace testing. All dimensions are in mm.*

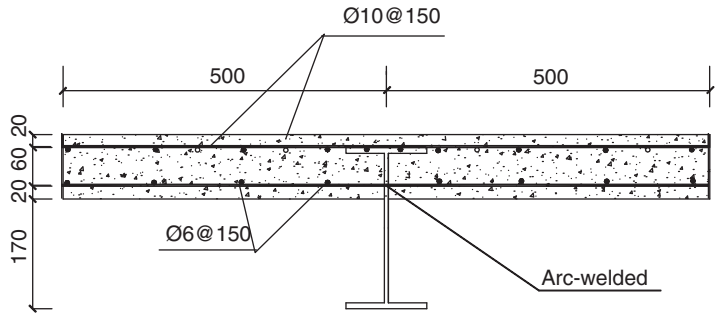

Figure 2. *Cross-section of the composite beam typical of a slim floor slab construction. The steel beam is embedded (partially) in the concrete slab. All dimensions are in mm.*

support a composite reinforced concrete (RC) floor slab with a partially embedded single floor beam (slim floor slab). Both columns were H section (H200 × 200 × 8 × 12) and were constructed from Q235 steel (Yield Strength 235 MPa). The steel beam (H section H250 × 125 × 6 × 9) was also made of Q235 steel. The frame height, measured from the base to the surface of the floor slab was 2800 mm. The center-to-center span length was 3600 mm.

The floor system was a typical slim floor slab construction, as the steel beam (upper flange and portions of the web plate) was embedded in the concrete slab. The 100 mm deep concrete floor slab was made of normal weight concrete (30–40 MPa). The cross-section of the composite beam with arrangement of reinforcing bars is shown in Figure 2. The frame described in [16,17] had a conventional slab construction, while the frame in the current article had a slim floor construction. The beam-to-column connections in the test frame were designed to transfer both moment and shear forces and were constructed with a 12 mm thick extended-end plate, bolted with eight, M22 Grade, 10.9 mm diameter bolt. Column bases were welded to a 16 mm thick steel plate, which was fixed to the test bed by four, M22 bolts. The frame was supported in the out of plane direction by three hollow steel pipes. These hollow steel pipes (extremely weak) are not expected to provide any restraint to the frame.

The furnace used to conduct the tests on full-scale structural frames under load was also identical to the one described in [16,17]. Vertical loading (using hydraulic jacks and load blocks) with constant load ratio 0.1 was identical to that used in tests with conventional floor slab construction, to enable a comparison of the experimental data with the various tests. The furnace test was conducted on two test frames. In one test, the beam-to-column connection was protected from furnace heating by an alumino-silicate refractory fiber blanket, while in the second test, both the columns and the beam-to-column connections were protected using a similar alumino-silicate

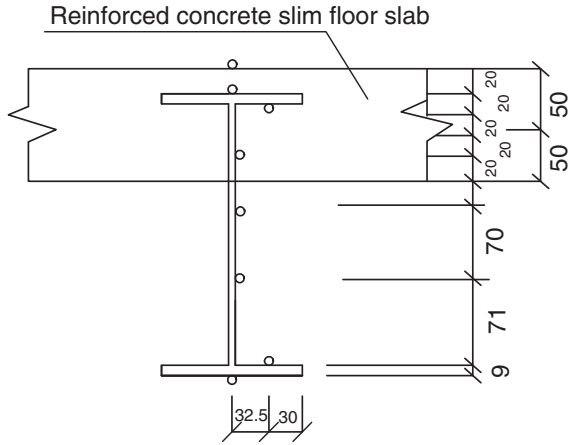

Figure 3. *Location of the thermocouples for the slim floor slab composite beam. All dimensions are in mm.*

refractory fiber blanket. The instrumentation of the test assembly, including the location of the thermocouples and the displacement transducers did not change from the configuration described in reference [16,17]. The only exception was the location of the thermocouples used to measure the temperature of the composite beam section. Eight K-type thermocouples were installed around the steel beam profile or embedded in the RC slab to measure the temperature distribution of the composite beam as shown in Figure 3. This difference in the instrumentation was primarily due to the slim floor slab construction discussed in this article. An uncertainty value of 5% was reported for the thermocouple temperature measurement [18], while the uncertainty in the displacement data was 3% [19].

EXPERIMENTAL RESULTS AND DISCUSSION

The furnace test was conducted on two test frames with slim floor slab construction to understand their response under fire conditions. The two test frames differed from each other in the protection on the columns from furnace heating. The experimental results for each test along with a brief explanation for the observed behavior are presented below.

As discussed earlier, a similar furnace test was conducted on two test frames with conventional floor slab construction and the results of those tests were reported in reference [16,17]. The two tests were referred to as Test 1 and Test 2 [16,17]. In Test 1, the beam-to-column connections were protected, while in Test 2 the columns as well as the beam-to-column connection were protected. Since the results of the current study will be compared and contrasted with

those described in [16,17], the two tests in the current study will be referred to as Test 3 and Test 4. In Test 3, the beam-to-column connection of the slim floor slab construction was protected, while in Test 4, both the columns as well as the beam-to-column connected was protected from furnace heating.

Figure 4 shows the composite beam section for conventional floor slab construction and the slim floor slab construction. The moment of inertia of the conventional floor construction (upper sub-figure) was $2.36 \times 10^8\,\text{mm}^4$, while that of the slim floor construction (down sub-figure) was $1.27 \times 10^8\,\text{mm}^4$. The bending moment capacity of the conventional floor was ~85% larger than that of the slim floor construction. Figure 4 also shows the relative location of the neutral axis in each type of construction. Due to the larger bending moment capacity of the conventional floor, one would expect the conventional floor slabs to perform better under fire loading and to have higher fire resistance rating. This article will examine the role of this large difference in bending moment capacity on the fire resistance rating of the conventional and slim floor slab construction.

The results for Tests 3 and 4 (utilizing slim floor slab construction) are described in detail in the following section. These results are compared and contrasted with each other and with those obtained in Tests 1 and 2

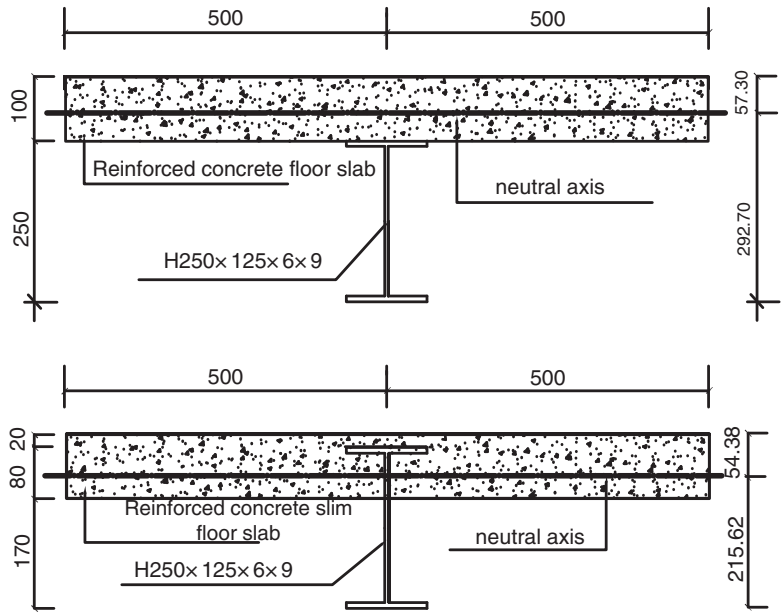

Figure 4. *Comparison of the moment of inertial of the composite beam for conventional floor construction (upper) and slim floor slab construction (down). All dimensions are in mm.*

(utilizing conventional floor slab construction) to understand the performance of slim floor and conventional floor slab construction, under fire loading.

Test 3 – Thermal and Structural Response

In Test 3, the beam-to-column connections of the composite steel frame with slim floor slab construction were protected from furnace heating by wrapping them in an alumino-silicate refractory fiber. The furnace was operated so as to replicate the temperature prescribed by the ISO 834 standard. Figure 5 shows the furnace temperature (symbols) plotted as a function of time measured by three thermocouples located at different points in the furnace. Data from the fourth thermocouple has not been presented, since it was found to be malfunctioning during this test. Figure 5 also shows the average temperature of the three thermocouples plotted as a function of time (solid line). On the average furnace temperature curve, nine critical points have been identified by a diamond symbol. These points were pre-selected and are important because the complete deformation of the structural frame will be presented at these nine critical points later in

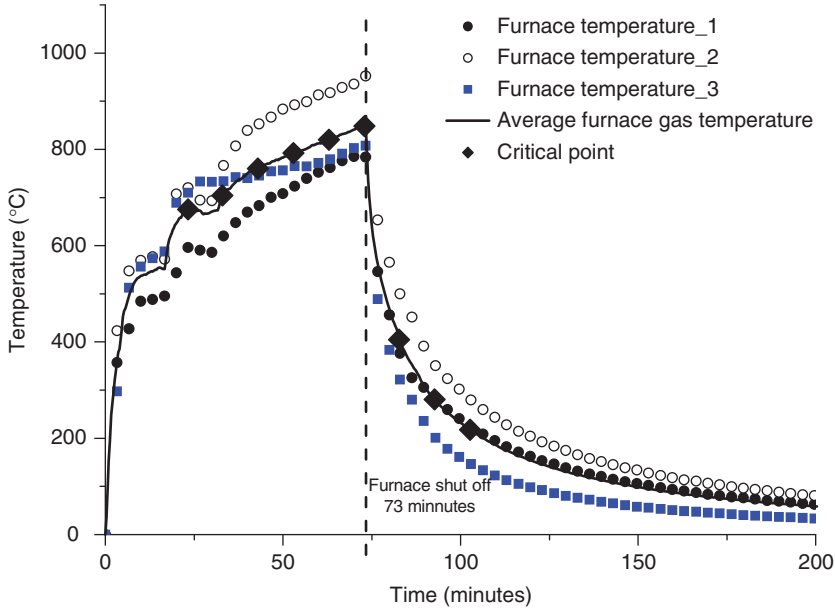

Figure 5. *Furnace temperature vs time for Test 3 measured at the same three thermocouple locations as in Test 1. Also shown is the average furnace temperature and the nine critical points (diamond symbol) at which the frame deformation is presented. (The color version of this figure is available online.)*

this article. For Test 3, structural failure (formation of a plastic hinge in column 1) was observed at 73 minutes after ignition at which point the furnace was shut down. Structural failure was identified by monitoring the rate of displacement (horizontal or vertical) as measured by the transducers, during the test. The temperatures recorded by the thermocouples at 73 minutes after ignition were 785, 949, and 809°C, respectively (Average temperature was 848°C). After shut down, the temperature of furnace gases reduced quickly as shown in Figure 5, and the test concluded at 200 minutes after ignition. For comparison, structural failure (due to formation of a plastic hinge) in Test 1 was observed 61 minutes after ignition and the average temperature at the shut-off point was 813°C.

Figure 6 shows the temperature plotted as a function of time at different locations along the composite beam cross-section. The thermal response of the composite beam section measured in Test 3 was considerably different from that measured in Test 1. This is because in a slim floor slab construction, a portion of the steel beam was partially embedded within the concrete floor. Since the top flange of the beam and portions of the web plate were protected from furnace heating by the RC slab, their temperature rose gradually as compared to that of the bottom flange. The difference between the top and bottom flange temperatures was ~600°C at 73 minutes

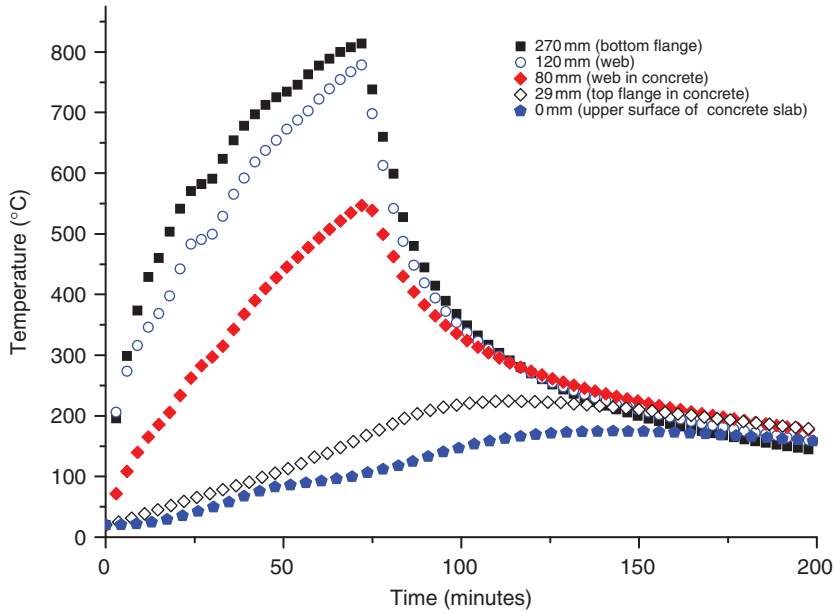

Figure 6. *Temperature distribution of composite beam. (The color version of this figure is available online.)*

after ignition (the time at which the furnace was shut-off). A comparison of these data with the experimental results obtained in Test 1 shows that the temperature difference between the top and bottom flange was only 221°C at the shut-off point. This result clearly shows that the upper flange temperature in Test 3 was significantly lower than that measured in Test 1. Experimental results also indicate that the temperature of the RC floor slab rose slowly as compared to the lower flange of the steel beam due to its large thermal mass. These differences in the measured thermal response influenced the deformation and failure time of the structure.

Figure 7 shows temperature profiles along the cross-section at seven different instants in time. The temperature is plotted as a function of distance measured from the top of the concrete slab. Profiles drawn at 20, 36, and 56 minutes after ignition represent the heat up phase, while those drawn at 79, 106, and 136 minutes after ignition represent the cool down phase. These results again indicate that during the heat up phase, the temperature of the upper flange was significantly lower than that measured in Test 1. This observation is important since the temperature distribution in the steel beam in Tests 1 and 3 influences the observed structural response, as discussed later in this article. The temperature through the cross section

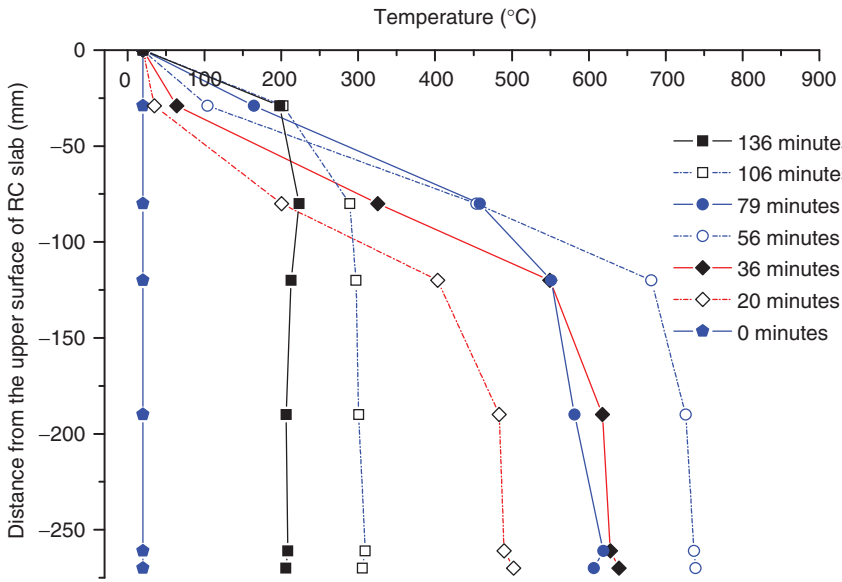

Figure 7. *Temperature as a function of distance (mm, measured from the top of the reinforced concrete (RC) floor slab) in the composite beam at different instants of time. (The color version of this figure is available online.)*

of the steel column as a function of time measured in Test 3 was similar to that measured in Test 1 [16,17].

Displacement Characteristics

This section discusses the measured horizontal and vertical displacement of the frame, during the heat up and the cool down phase. Heating of the structural frame results in thermal expansion of the various structural components, and restrained thermal expansion can result in thermally induced stresses and deformations of the frame.

The horizontal displacements at top and mid-height for column 1 and column 2 plotted as a function of the average furnace temperature are shown in Figure 8, while the same horizontal displacements are plotted as a function of time in Figure 9. As the composite floor slab expands, columns 1 and 2 are pushed apart in opposite directions. Results indicate that the horizontal displacements increased linearly until the average fire temperature reached 450°C. During this initial heating phase, the deformation of columns 1 and 2 was outwards and symmetric and the displacements at top and at mid-height of columns were almost equal. When the average furnace temperature was below 450°C, the temperature gradient in the concrete slab and the floor beam was such that it induced bowing of the floor slab downwards towards the furnace. Since the column temperature was only

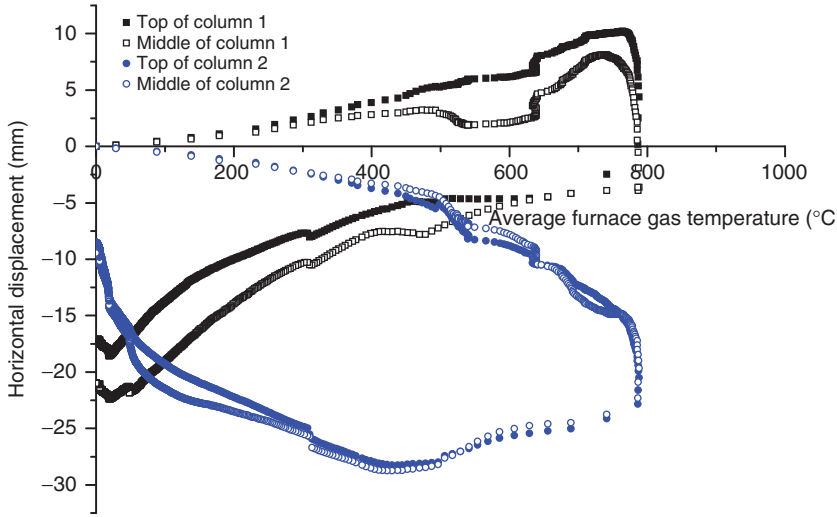

Figure 8. *Horizontal displacements measured for columns 1 and 2 as a function of average furnace temperature. (The color version of this figure is available online.)*

151°C, there had been very little degradation of the steel strength until this point, and as a result the columns were very stiff and provided significant restraint to thermal expansion of the composite beam.

As the average furnace temperature rose above 450°C, the displacements become asymmetric and highly nonlinear. This is attributed to thermal degradation of material properties at high temperatures as well as to the combination of moment and axial force of steel column. Figure 9 clearly shows buckling of column 1 at ~73 minutes after ignition, which results in an asymmetry in the displacement curve. At this point, the maximum horizontal displacement at the top of columns 1 and 2 are 10.0 and 19.0 mm, respectively. Although the loading on both columns was similar, column 1 buckled before column 2 due to slight imperfections in the loading. Once column 1 buckled, the furnace was shut-off, and as a result, buckling of column 2 was prevented. In Test 3, column 1 buckled first, and the movement of the test frame was towards column 2. On the other hand, in Test 1, column 2 buckled first, and the movement of the test frame was towards column 1. In both Test 1 and Test 3, run-away failure was predicted as both columns moved in the same direction. Column failure in Test 1 occurred at 61 minutes after ignition, while in Test 3, failure was observed at 73 minutes after ignition. Comparison of the results for Tests 1 and 3 indicate that the fire resistance of a slim floor slab construction is at least as good, if not better than that of a conventional floor construction. During the cool down phase, the displacement for

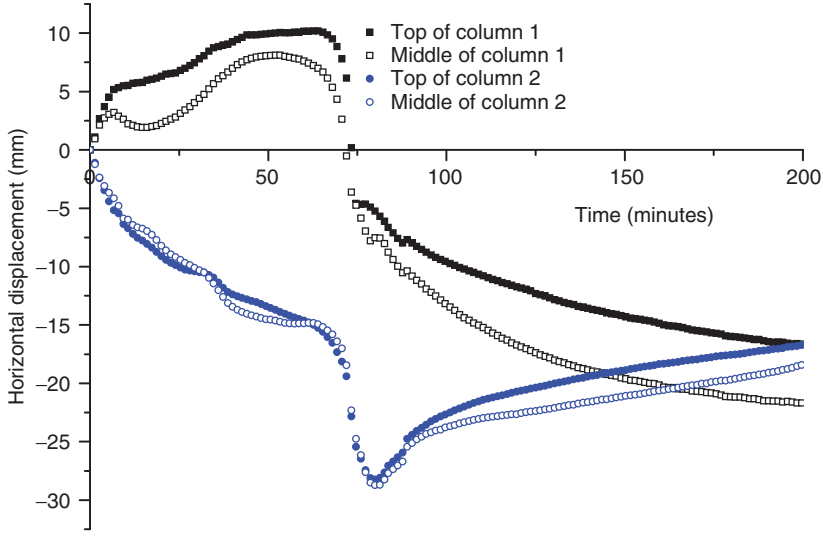

Figure 9. *Horizontal displacement measured for columns 1 and 2 plotted as a function of time. (The color version of this figure is available online.)*

columns 1 and 2 were asymmetric, this is attributes to the column local buckling and indicating the importance of conducting the tests during the heating and the cooling phase. At the conclusion of the experiment, the top of columns 1 and 2 had displacement residual values of 16.6 and 16.7 mm, respectively, as shown in Figure 8.

As the composite floor was heated, the floor sagged due to loss of material stiffness and constrained thermal expansion. The main reason for the sagging was the thermal gradients in the section. The mid-span deflection of the composite beam plotted as a function of time is shown in Figure 10. The floor deflection increased linearly during the heating phase until the average furnace temperature reached 450°C. Beyond 450°C, the behavior of the floor slab was highly nonlinear and asymmetric. The floor deflection was 35.3 mm at 73 minutes after ignition. At the point when column 1 buckled, the deflection changed dramatically. After the furnace was shut-off, the deflections reduced and a residual value of 18.7 mm was observed for the mid-span deflection at the conclusion of the test.

Figure 11 shows the complete process of deformation of the test frame during the heating and cooling phase at the nine critical instants in time. These nine critical points were shown in Figure 5. Each sub-figure corresponds to one of these critical points on the furnace heating/cooling cycle. Out of the nine selected time values, six occurred in the heating phase,

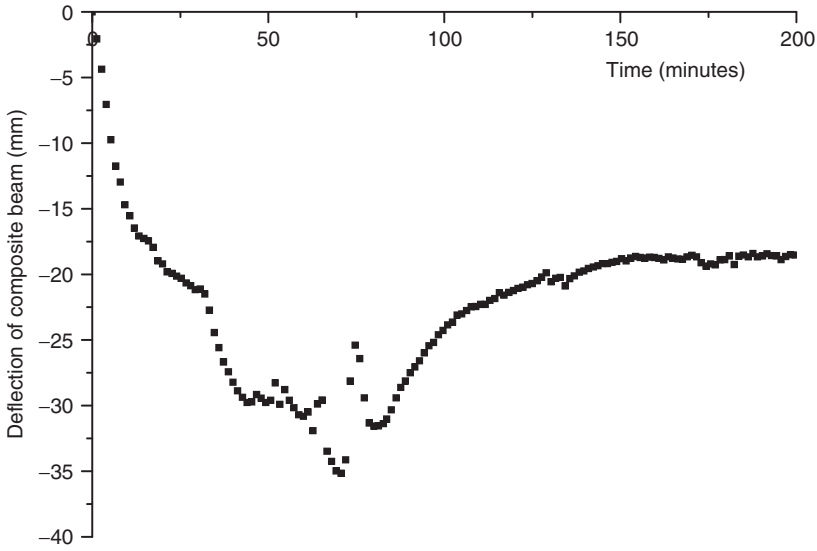

Figure 10. *Vertical deflection of composite beam (mid-span location) plotted as a function of time.*

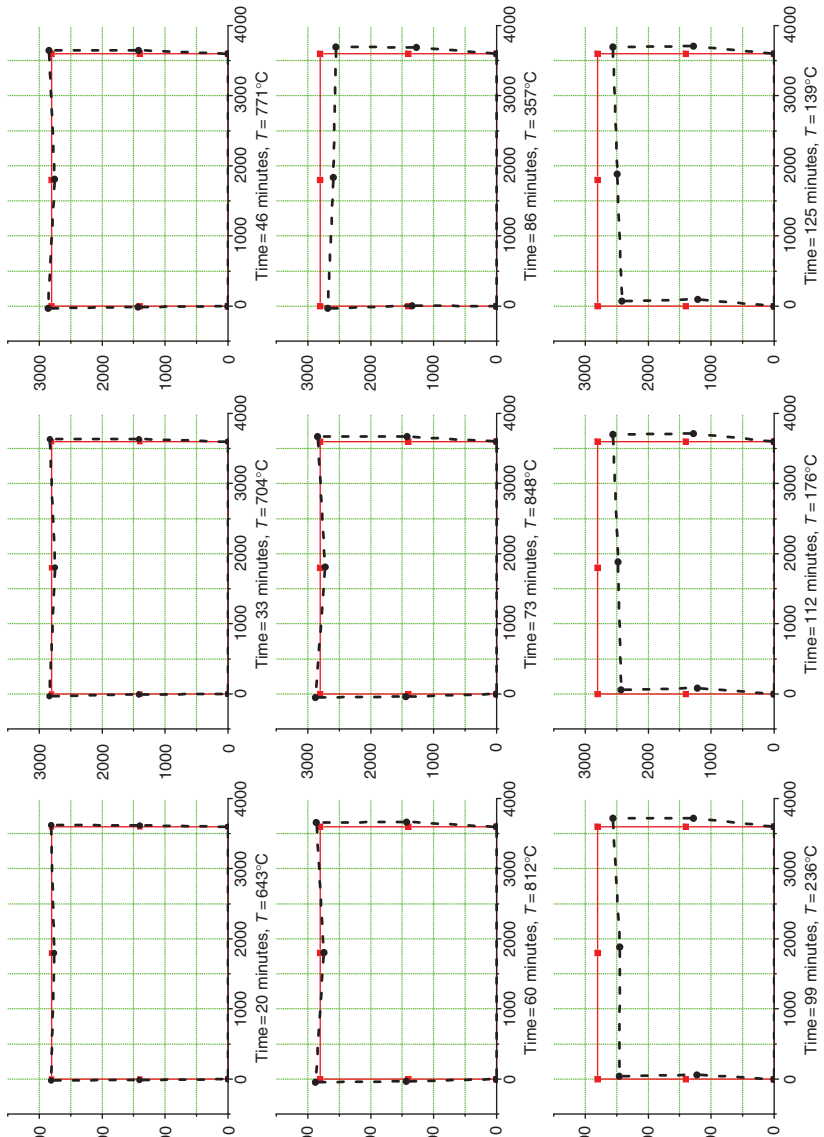

Figure 11. *Deformation illustration of composite frame at nine different instants in time. (The color version of this figure is available online.)*

while three occurred in the cool down phase. Results indicate that the displacement of the test frame was almost symmetric during the heating phase as the columns were pushed out by the floor system. However, when column 1 buckled, the deformation of the test frame became asymmetric. After the furnace was shut-off, the displacement of column 1 and 2 were in the same direction and were increasing with time implying that the frame was undergoing run-away failure. Note that the displacements shown in Figure 11, have been magnified eight times to improve visibility, since the actual values of the displacement were small compared to the dimensions of the frame. This level of magnification is consistent with that used for the corresponding figure in reference [16,17].

Once the furnace temperature reached its ambient value, the frame was removed from the furnace and examined for visual signs of local failure. Figure 12 shows a photograph of the test frame after it was removed from the furnace. This photograph corresponds to the last sub-figure in Figure 11. Visual observations clearly indicate the formation of a plastic hinge on column 1 close to the connection with the composite floor. Test 1 indicated a similar kind of failure on column 2. Occurrence of the column local buckling was attributed to flanges lost their stability in the vicinity of the connections at the high furnace temperatures. Since the beam-to-column connections were protected from furnace heating and the composite beam was stiffer

Figure 12. *Photograph of the frame at the conclusion of the furnace test showing the formation of local buckling on column 1 close to the connection. (The color version of this figure is available online.)*

than the column, plastic hinge formed in the column underneath the joint. The photograph also indicates bowing of the column and vertical deflection of the composite beam.

Figure 13 shows the formation of cracks in the RC floor slab, observed when the frame was removed from the furnace for inspection. Cracks along the width of the slab were concentrated near the beam-to-columns connection, while fewer cracks were observed in the mid-span section. Inspection of the concrete slab at the conclusion of Test 1 had also indicated concentration of cracks near the beam-to-column connection. In addition, the concrete slab in Test 1 indicated the presence of diagonal cracks, near the beam-to-column connection. Such diagonal cracking was not observed in Test 3. In Test 1, the steel beam was connected to the slab through shear studs, while in Test 3, the steel beam was embedded in the concrete slab and was welded to the reinforcing bars. The presence of diagonal cracks in Test 1 and not in Test 3, can be explained by the manner in which load is transferred from the beam to the slab for composite action. In a conventional slab construction, stresses are concentrated in a small region around the studs, and are not distributed uniformly through the width of the slab, resulting in the diagonal cracks. When the beam was embedded in the slab and was welded to the re-inforcing bars, as in a slim floor slab construction, the load transfer was more uniform through the width of the slab. This results in perfectly parallel cracks running along the width of the slab as seen in Figure 13. It was also noted that more cracks were observed in Test 3 as compared to Test 1. Comparison of the crack pattern in the concrete slab following Tests 1 and 3 indicates that the composite floor action was achieved to a higher degree in a slim floor construction as compared to a conventional floor slab construction.

Test 4: Thermal and Structural Response

The primary difference between Tests 3 and 4 was the manner in which heat was applied to the columns of the test frame. In Test 3, the beam-to-column

Figure 13. *Photograph of the reinforced concrete floor slab at the conclusion of the furnace test. (The color version of this figure is available online.)*

connection alone was protected from furnace heating, while in Test 4, the column as well as the beam-to-column connections were protected from furnace heating. Tests 2 and 4 have similar protection around the structural members, but differ in the construction of the test frame. Test 4 is slim floor slab construction while Test 2 described in reference [16,17] was conventional floor slab construction. Experimental results for Test 4 are discussed in detail in this section and are compared with those for Test 3 (reported earlier) to understand the role of heating. The results for Test 4 are also compared with those for Test 2 to understand fire resistance of slim floor slab construction as compared with conventional floor construction.

Figure 14 shows the furnace temperature plotted as a function of time and measured by the two thermocouples. The average furnace temperature plotted as a function of time has also been indicated with a solid line. As in Test 3, nine critical time levels were selected and marked on the average furnace temperature versus time curve. These critical points are important since the full frame deformation will be discussed at these time levels, later in this article. For Test 4, structural failure (local buckling) was observed at 89 minutes after ignition, and the furnace was shut-off at that point. At this point, the average gas phase furnace temperature value was 1026°C.

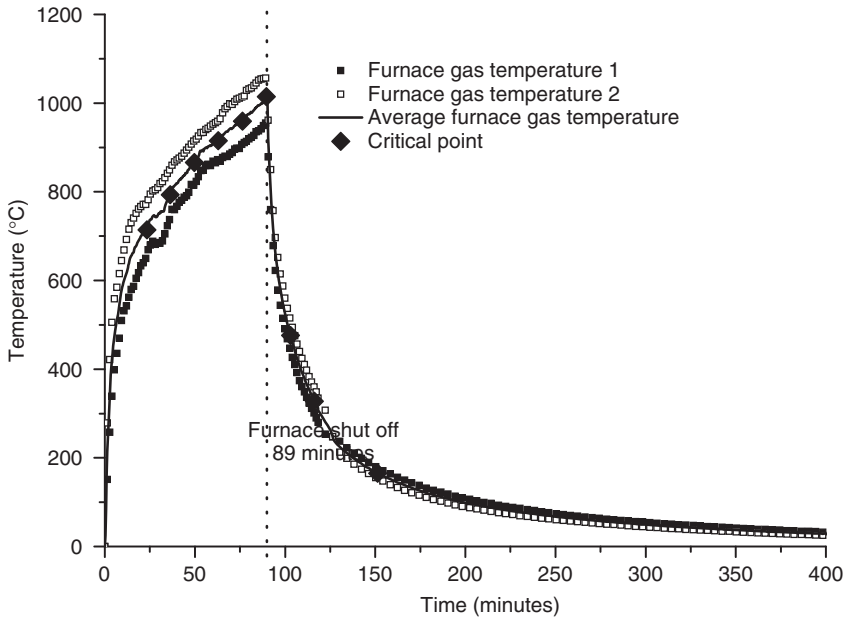

Figure 14. *Furnace gas temperature measured as a function of time for Test 4. Also shown is the average furnace gas temperature and the nine critical points (diamond symbols) for which frame deformation is presented in Figure 18.*

After furnace shut down, the temperature of the furnace gases reduced quickly as shown in Figure 14, and the test concluded at 400 minutes after ignition. As a comparison, structural failure (local bucking) in Test 2 was observed at 88 minutes after ignition.

The composite beam and the concrete slab heat up in a manner similar to that for Test 3. However, since the columns were protected from furnace heating, the columns in Test 4 do not heat up significantly. Due to the differences in heating of the frame in the two tests, the measured horizontal displacements of the column and the vertical deflections of the composite beam shows a completely different response to the imposed loads.

Figure 15 shows the variation of the horizontal displacements of each column plotted against the average furnace temperature, while Figure 16 shows the same horizontal displacements plotted against time. Each figure shows the horizontal displacements as measured by the transducers located at the middle and top of the two columns. In general, the horizontal displacements were much smaller than those observed for Test 3. Results indicate that below 480°C, the horizontal displacement increases linearly with average furnace temperature. The displacements of columns 1 and 2 were symmetric, and the columns were being pushed outwards due to the expansion of the composite beam. Beyond 480°C, the horizontal displacements of the columns become highly nonlinear function of average furnace

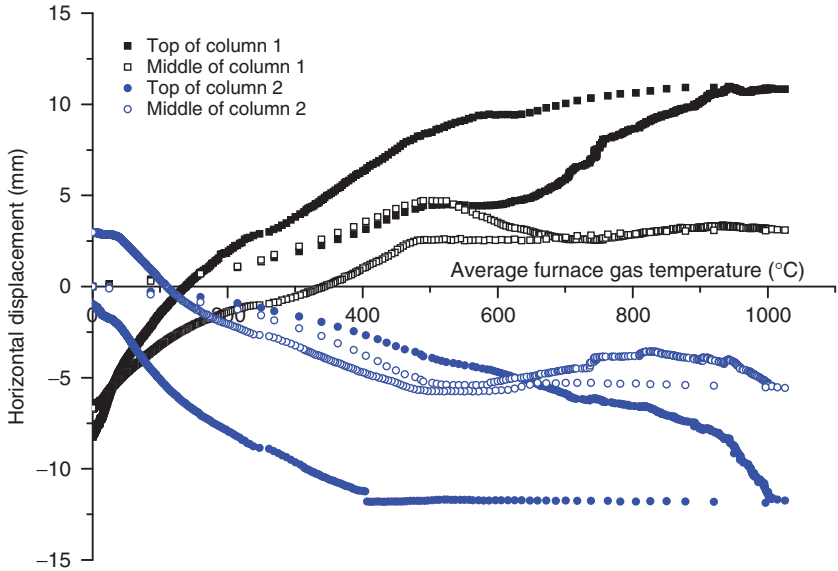

Figure 15. *Horizontal displacement of columns (Test 4) plotted as a function of average furnace temperature. (The color version of this figure is available online.)*

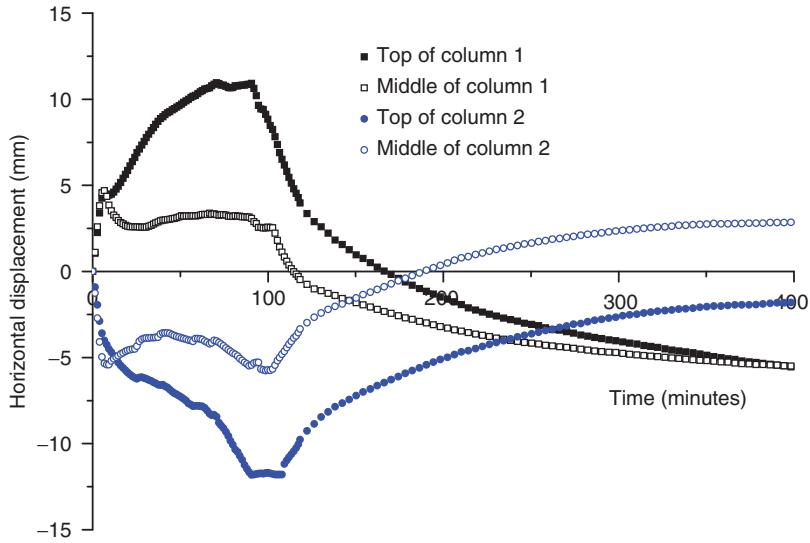

Figure 16. *Horizontal displacement of columns (Test 4) plotted as a function of time. (The color version of this figure is available online.)*

temperature due to bowing of the composite beam and material degradation at high temperatures. The furnace was shut-off at 89 minutes after ignition. At this point, the maximum horizontal displacement values for columns 1 and 2 were 10.8 and 11.9 mm, respectively.

Local buckling of the floor beam in Test 4 was observed at 89 minutes after ignition, while column buckling was observed in Test 3 at 73 minutes after ignition. Results for Test 4 do not indicate the run-away failure that was observed in Test 3. This indicates that for the slim floor slab construction studied during these tests the fire resistance rating of the composite beam was better than that of the column. A similar result was obtained for conventional floor slab construction [16,17]. Horizontal displacement data measured in Test 4 indicate a behavior very similar to that measured in Test 2. Local buckling of the steel beam was observed in Test 2 at 88 minutes after ignition and in Test 4 at 89 minutes after ignition. These results again indicate that the fire resistance of slim floor slab construction is at least as good as that of conventional floor slab construction.

Figure 17 shows the composite beam vertical deflection plotted as a function of time. The reader is referred to [16] for a discussion of how the deflections were computed from the results of the displacement transducer. As observed for the columns, the deflections increased linearly until 490°C. Beyond 490°C, beam deflections were highly nonlinear, and were dominated by high temperature material nonlinearites and the

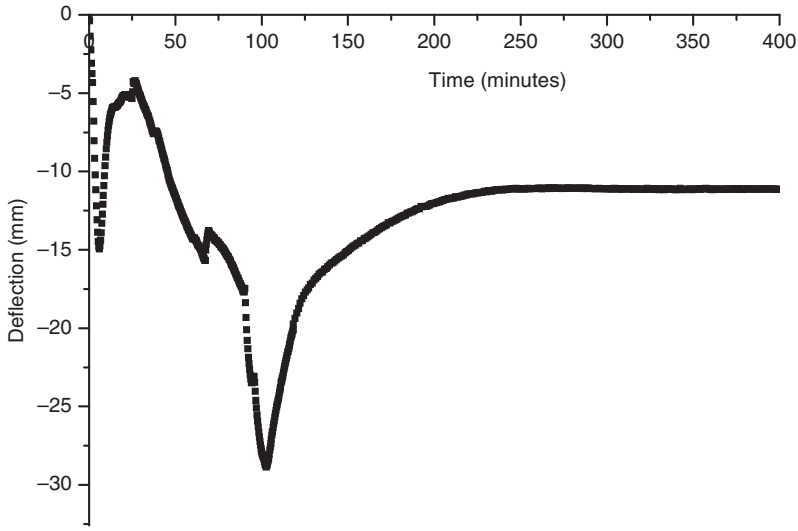

Figure 17. *Vertical deflection of composite beam (Test 4) plotted as a function of time.*

restraining action of the columns. There was a short reversal in beam deflection observed between 7 and 27 minutes after ignition. This reversal was likely due to the restraining action provided by the columns (the columns were protected in Test 4, and were at a lower temperature). Such a reversal in beam deflection was not observed in Test 3, since the columns in that test were not protected and did not provide the same level of restraining action on the beam. Detailed numerical modeling of this experiment will help in further understanding the observed reversal in the beam deflection curve, shown in Figure 17. Beam deflections reached a maximum deflection value of 28.9 mm during the cool down phase, well after the furnace was shut-off. A residual value of 11.1 mm was observed at the end of the cool down phase. The vertical deflection plot shows a trend that is similar to that obtained in Test 2.

Figure 18 shows the complete process of deformation during the heat up and the cool down phase plotted based on data collected by the displacement transducers. As in Test 3, each sub-figure in Figure 18 corresponds to one of the nine critical instants in time, shown in Figure 14. The first seven time instants occurred in the heat up phase while the last two occurred in the cool down regime.

Results indicate that in both the heating phase and the cooling phase, the deformations of the columns were almost symmetric. During the heating phase, the columns were pushed outwards, however, when the test frame

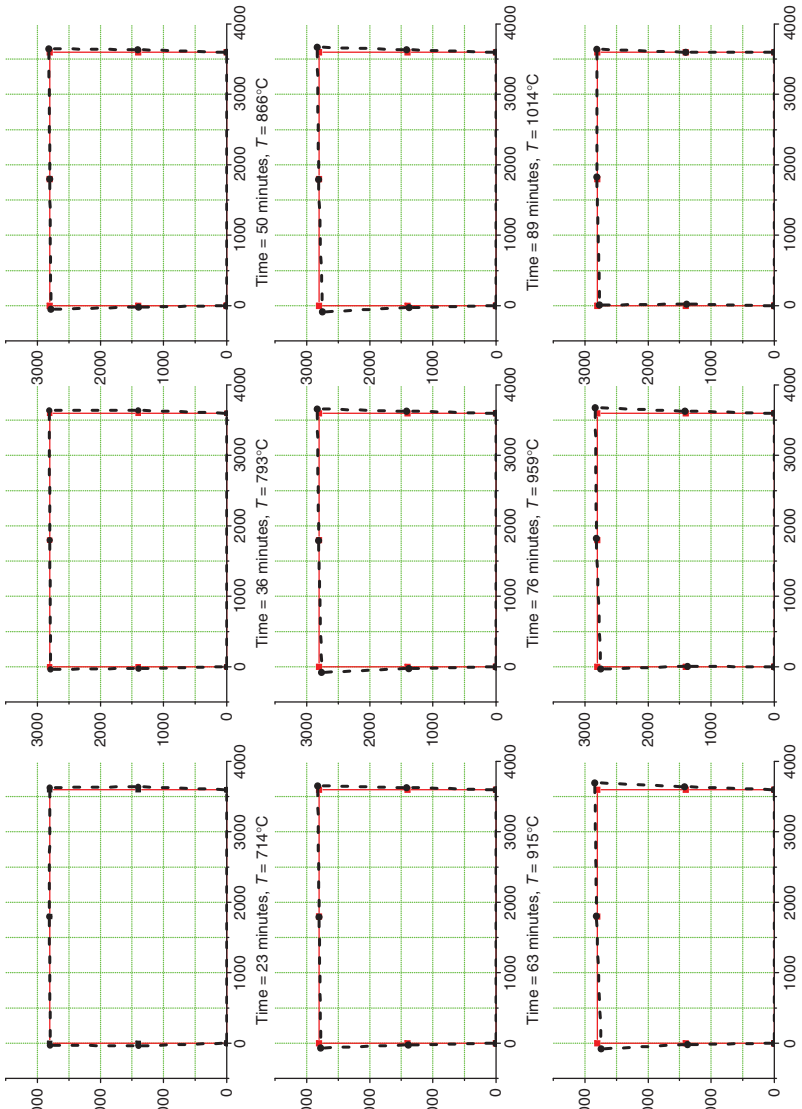

Figure 18. *Deformation of composite frame at nine different instants in time. (The color version of this figure is available online.)*

Figure 19. *Photograph of the frame at the end of Test 4 showing local buckling of the steel beam. (The color version of this figure is available online.)*

cools down completely, the columns at mid-height were being pulled inwards (towards each other). The vertical beam deflection increases during the heat up phase and reduced during the cool down phase. Since the frame displacements were very small compared to the dimension of the test frame, the displacement values have been amplified by a factor of eight to improve visibility.

Following the cool down phase, the frame was removed from the furnace and was visually inspected for signs of local failure. Figure 19 is a photograph of the frame after it was removed from the furnace. Since the columns and the beam-to-column connection were protected from furnace heating, Figure 19 shows local buckling on the beam web at about 100–600 mm from the end plate close to column 1. Examination of the concrete slab also indicates the presence of cracking similar to that observed in Test 3.

Comparison of the experimental results for Tests 3 and 4 clearly indicates the importance of protecting the columns from furnace heating. In Test 3, where the columns were not protected from furnace heating, structural failure was observed at 73 minutes after ignition followed by run-away failure during the cool down phase. On the other hand, in Test 4, where the columns were protected from furnace heating, local buckling was observed at 89 minutes after ignition, but run-away failure was not observed. A similar behavior was observed when the results of Test 1 were compared with those of Test 2.

Experimental data for Tests 1–4 (summarized in Table 1) indicates that the fire resistance of a slim floor slab construction is at least as good as that for a conventional floor slab construction. As discussed earlier the bending moment capacity of a conventional floor slab was 85% higher than that of a slim floor slab construction. This implies that the conventional floor slab construction should be better able to resist fire loads. However, the fire

Table 1. Comparison of test conditions and failure modes observed in Tests 1–4; results for Tests 1 and 2 were discussed in reference [16,17].

Test no.	Test 1	Test 2	Test 3	Test 4
Test Frame	Conventional slab	Conventional slab	Slim slab	Slim slab
Protection from furnace heating	Beam-to-column connections	beam-to-column connections and columns	beam-to-column connections	beam-to-column connections and columns
Temperature (average) at shut-off	813°C	868°C	851°C	1026°C
Failure mode	Buckling of column 2	Local buckling of beam	Buckling of column 1	Local buckling of beam
Time to failure	66 minutes	88 minutes	71 minutes	89 minutes
Run-away failure	Yes – column 2	No	Yes – column 1	No
Post-test frame inspection	Plastic hinge – column 2	Local buckling of beam	Plastic hinge – column 1	Local buckling of beam
Post-test slab inspection	Diagonal cracks	Diagonal cracks	Parallel cracks	Parallel cracks
Relative fire performance		Better than Test 1	As good as Test 1	As good as Test 2. Better than Test 3

resistance of a slim floor construction was as good as that of a conventional floor slab because of the differences in the thermal protection provided by the concrete slab to the steel beam. In a slim floor slab construction, the portion of the steel beam that is partially embedded in the concrete slab does not heat up as significantly as the portion that is fully exposed to furnace heating. The thermal protection provided by the concrete slab to the steel beam is the primary reason for the better fire resistance of a slim floor slab construction, as compared to conventional floor slab construction.

CONCLUSIONS AND RECOMMENDATION

A furnace test was carried out on two full-scale composite steel frames with slim floor slab construction to understand their response under fire heating scenarios. In one frame the beam-to-column connections were protected, while in the second frame, the columns as well as the beam-to-column connections were protected. Test results including thermocouple temperature measurement as well as displacement data was presented.

Based on these tests, it is noted that the fire resistance rating of a composite beam is better than that of the column examined in the current set of full-scale composite frame experiments. This suggests that typical building structures using similar elements and connections should have protected columns with sufficient insulation to limit their deflections, while the composite beams may require less or no insulation because of their better performance under furnace test. Test results indicate that the fire resistance of the slim floor slab construction tested was at least as good as that of the conventional floor slab construction due to the thermal protection provided by the concrete slab to the embedded portion of the steel beam. Comparison of the crack pattern in the concrete slab for the various tests indicates that the composite floor action was achieved to a higher degree in a slim floor construction as compared to a conventional floor slab construction.

It is proposed that a comprehensive modeling effort involving thermal and structural analysis should be undertaken to fully understand the experimental results and to gain a better understanding of the fire induced structural response of frames with slim floor slab construction.

ACKNOWLEDGMENTS

This project was supported by the NSFC with Grant No. 50878069, the China MOST with Grant No. 2006BAJ13B03 and HZ2008-KF03, and one of the authors (Y. Dong) deeply appreciated their support.

REFERENCES

1. Bailey, C.G., "The Behaviour of Asymmetric Slim Floor Beams in Fire," Journal of Constructional Steel Research, Vol. 50, No. 3, 1999, pp. 235–257.
2. Lu, X. and Makelainen, P., "Slim Floor Development in Sweden and Finland," Structural Engineering International, Vol. 6, No. 2, 1996, pp. 127–129.
3. Newman, G.M., "Fire Resistance of Slim Floor Beams," Journal of Constructional Steel Research, Vol. 33, No. 1–2, 1995, pp. 87–100.
4. Ma, Z. and Mäkeläinen, P., "Behavior of Composite Slim Floor Structures in Fire," Journal of Structural Engineering, Vol. 126, No. 7, 2000, pp. 0830–0837.
5. Najjar, S.R. and Burgess, I.W., "A Nonlinear Analysis for Three-dimensional Steel Frames in Fire Conditions," Engineering Structure, Vol. 18, No. 1, 1996, pp. 77–89.
6. Bailey. C.G. and Moore, D.B., "The behavior of Full-scale Framed Buildings Subject to Compartment Fires," The Structural Engineer, Vol. 77, No. 8, 1999, pp. 15–21.
7. Usmani, A.S., Rotter, J.M., Lamont, S., Sanad, A.M. and Gillie, M., "Fundamental Principles of Structural Behavior under Thermal Effects," Fire Safety Journal, Vol. 36, No. 8, 2001, pp. 721–744.
8. Buchanan, A.H., Structural Design for Fire Safety, New York, John Wiley & Sons, Inc., 2001.
9. BSI 476, Fire Tests on Building Materials and Structures Part 20: Method for Determination of the Fire Resistance of Elements of Construction (General Principles), London, British Standards Institution, 1987.
10. Franssen, J.M., Talamona, D., Kruppa, J. and Cajot, L.G., "Stability of Steel Columns in Case of Fire: Experimental Evaluation," ASCE Journal of Structural Engineering, Vol. 124, No. 2, 1998, pp. 158–163.
11. Liu, T., "Experimental Investigation of Behavior of Axially Restrained Steel Beams in Fire," Journal of Constructional Steel Research, Vol. 58, No. 9, 2002, pp. 1211–1230.
12. Wald, F., Simões da Silva, L., Moore, D.B., Lennon, T., Chladna', M., Santiago, A., Benes, M. and Borges, L., "Experimental Behavior of a Steel Structure under Natural Fire," Fire Safety Journal, Vol. 41, No. 7, 2006, pp. 509–522.
13. Zhao, J.C. and Shen, Z.Y., "Experimental Studies of the Behavior of Unprotected Steel Frames in Fire," Journal of Constructional Steel Research, Vol. 50, No. 2, 1999, pp. 137–150.
14. Wastney, C., Performance of Unprotected Steel and Composite Steel Frames Exposed to Fire. Project Report, Department of Civil Engineering, University of Canterbury, Christchurch, New Zealand, 2002.
15. Liew, J.Y., Tnng, L.K., Holmaas, T. and Choo, Y.S., "Advanced Analysis for the Assessment of Steel Frames in Fire," Journal of Constructional Steel Research, Vol. 47, No. 1, 1998, pp. 19–45.
16. Dong, Y. and Prasad, K., Large Scale Experiments on Structures under Fire Loading. 1. Behavior of Full-scale Composite Frames with Conventional Floor Slab under Furnace Loading. NISTIR 7394, National Institute of Standards and Technology, Gaithersburg, MD USA, 2007.
17. Dong, Y. and Prasad, K., Large Scale Experiments on Structures under Fire Loading. 2. Behavior of Full-scale Composite Frames with Slim Floor Slab under Furnace Loading. NISTIR 7400, National Institute of Standards and Technology, Gaithersburg, MD USA, 2007.
18. Jiang, Z. and Chen, X., Measurement and Control of Temperature. Press of Tsinghua University, Beijing, 2005.
19. Li, K., New Manual of Transducer Technology. National Defense Industry Press, Beijing, 2002.